Article citation info:
Noga M, Moskal T. Evaluation of a pressure sensing glow plug in terms of its application possibility to control the combustion process of a hydrogen-powered spark-ignition engine. Combustion Engines. 2024;196(1):140-145. https://doi.org/10.19206/CE-172820

Marcin NOGA
Tomasz MOSKAL

Combustion Engines
Polish Scientific Society of Combustion Engines

Evaluation of a pressure sensing glow plug in terms of its application possibility to control the combustion process of a hydrogen-powered spark-ignition engine

Article Info

Received: 2 June 2023
Revised: 14 September 2023
Accepted: 22 September 2023
Available online: 11 November 2023

The article contains the results of an analysis of the suitability of a pressure sensing glow plug for use in a hydrogen engine control system. Due to the properties of hydrogen, the process of its combustion in spark-ignition engines is significantly different from the classic fuels. It is planned to use the pressure sensor signal to control the combustion process to obtain high power and efficiency, with the lowest possible emission of nitrogen oxides, which is the main harmful component of hydrogen engines. After an initial assessment of suitability, it was decided to use a pressure sensing glow plug. This choice is dictated by the low price, good availability and high durability of these sensors. The preliminary tests were carried out using a low-power single-cylinder SI engine coupled with a 48 V generator. The tests were carried out for several values of engine speed and load of the generator and for classic gasoline with a research octane number (RON) of 95. To obtain an increased pressure rise rate in the cylinder, as for hydrogen fueling, the engine operation was also tested with unmodified light gasoline used as solvent, which is characterized by a significantly lower RON value. The use of a reference pressure sensor in the cylinder made it possible to determine the behavior of the PSG in various operating conditions. The tests revealed that the differences in the pressure waveforms registered with both sensors can be systematized depending on the engine speed and its load.

Key words: *pressure sensing glow plug, in-cylinder pressure, engine control, spark ignition, hydrogen fuel*

1. Introduction

Fossil fuel depletion and stricter emission regulations drive the search for alternative fuels that can both meet the pollution requirements but still be suitable for piston engines that still developed [19], and are in a majority of vehicles currently in use not only for road transport [9], but also, to a large extent, in rail transport [3, 14].

Various types of alternative fuels are still being developed to decrease emissions [2, 15, 16], although uniquely hydrogen is a fuel that inherently does not produce carbon-related emissions when combusted, thus serving as a suitable substitute to classic liquid fuels [5, 7, 8, 21]. The combustion of hydrogen still requires minimization of nitrogen oxide emissions, and the distinct nature of hydrogen as a fuel in comparison to gasoline requires advanced control methods to enhance the efficiency of the process. Table 1 presents a comparison of fuel properties according to [1, 18].

Table 1. Comparison of hydrogen and gasoline properties as a fuel

Parameter	Unit	Hydrogen	Gasoline
Density	kg/m^3	0.090 (gas)	735
Lower Heating Value (LHV)	MJ/kg	120.1	44
LHV of stoichiometric mixture	MJ/kg	3.4	2.81
Laminar flame speed	m/s	2.4	0.4
Stoichiometric air-fuel ratio (AFR)	kg/kg	34.3	14.7
Research octane number	–	130	95
Diffusion coefficient in air	cm^2/s	0.61	0.05
Minimum energy of ignition in air	mJ	0.02	0.24
Self-ignition temperature	K	858	510–744
Flame temperature in air	K	2318	2470
Flammability range (relative AFR)	–	0.14–10	0.3–1.67

Advanced combustion control methods, also known as smart combustion control, have already been approached, with tailored pressure sensors for this purpose [4, 20].

To achieve a similar goal, an application of in-cylinder pressure signal is proposed with the use of a pressure-sensing glow plug, commonly found in current diesel engines, making it a lower-cost alternative to bespoke sensor systems.

The PSG of choice was the PSG006 sensor made by BERU (BorgWarner). To evaluate its suitability and extend previous research on applying a PSG as a stand-alone pressure sensor [6, 17], a comparative study against a laboratory-grade pressure sensor – Optrand D822D6-SP – has been conducted. Tables 2 and 3 present the available technical data for the sensors used.

Table 2. Beru PSG parameters as per [10]

Parameter	Unit	Value
Pressure range	bar	0–200
Accuracy	–	±2%
Resolution	steps/cycle	700
Sensor principle	–	piezo-resistive

Table 3. Optrand D822D6-SP parameters [11]

Parameter	Unit	Value
Pressure range	psi (bar)	0–1500 (0–100)
Sensitivity	mV/psi (mV/bar)	2.66 (38.58)
Sensor principle	–	optical

2. Test stand

As part of the research topic, it is planned to use the PSG sensor for a four-cylinder liquid-cooled engine. Since testing the suitability of the sensor requires two pressure sensors to be mounted together in the engine combustion chamber, it was decided to use a low-power single-cylinder air-cooled engine for the initial stage of the research. The engine selected for the tests was used to drive the 48 V-range extender developed a few years ago at the Cracow University of Technology [12, 13]. The range extender is

attached to a light commercial electric vehicle Melex and can charge its traction battery. The view of the test stand based on the engine of the range extender developed for the Melex vehicle is shown in Fig. 1.

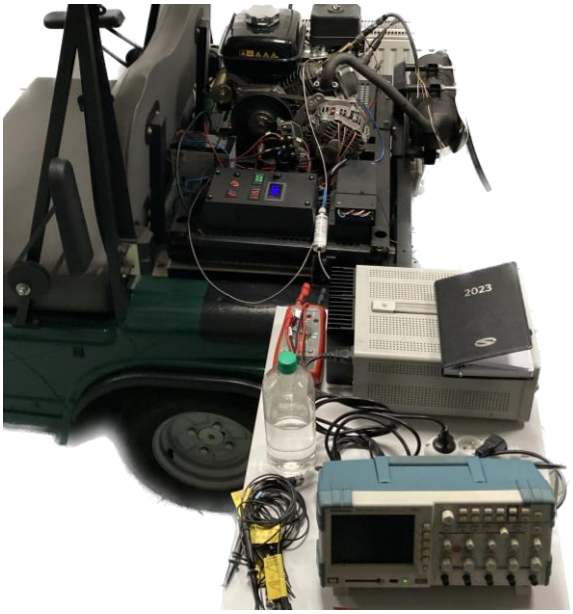

Fig. 1. Test stand consisting of a Melex cart with a range extender ICE

Charge current can be set via a regulator mounted next to the engine. This allows smooth adjustment of the engine load. Maintaining a constant engine speed is carried out by a centrifugal governor. The main technical specifications of the range extender are presented in the Table 4.

Table 4. Range extender technical data

Engine model	WEIMA 168FA
Engine type	four-stroke, SI, single cylinder
Engine displacement	163 cm^3
Engine maximum power	3.8 kW at 3600 rpm
Ignition timing	fixed, 27°CA BTDC
Generator type	Synchronous 3-phase AC
Nominal voltage	48 V
Continuous output power	2200 W
Peak overall efficiency	18.8%

During the tests, the actual ignition timing was also measured for various engine speeds. The angle of ignition is fixed and set to 27°CA BTDC which is a slightly higher value than declared in the available technical specifications of the engine (25°CA BTDC).

The engine was equipped with a crank angle sensor and two in-cylinder pressure sensors – a BorgWarner PSG and an Optrand D822D6-SP (Fig. 2 and Fig. 3).

Fig. 2. PSG mounted inside the spark-plug fitting adapter next to a PSG

Fig. 3. Tip view of the PSG next to the adapter

To install the pressure sensors, a brass adapter (Fig. 2) has been designed and manufactured at Cracow University of Technology. The glow plug seals on its conical surface inside the adapter. The adapter has an axial channel to house the tip of the glow plug, as seen in Fig. 3. A threaded channel on a side wall of the adapter has been prepared, to provide a fitting for the reference sensor. Both channels form a single volume so that both sensors face the same pressure conditions. The equipped adapter is shown in Fig. 4.

Fig. 4. Both sensors fitted to the adapter

The adapter with two pressure sensors has been mounted into the factory spark plug fitting, while the spark plug itself has been installed in an additional fitting that was made in the cylinder head for the installation of a second spark plug as part of previous research and development, as shown in Fig. 5.

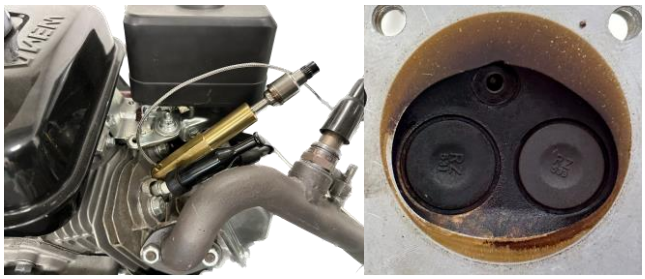

Fig. 5. Adapter mounted to the cylinder head. Note: combustion chamber view (right) does not show the additional spark plug fitting – a standard cylinder head shown

Pressure sensors are supplied by a linear power supply. Sensor readings were observed through a 4-channel digital oscilloscope Tektronix TPS2024 and registered onto external memory for further processing. A diagram of the test stand is presented in Fig. 6.

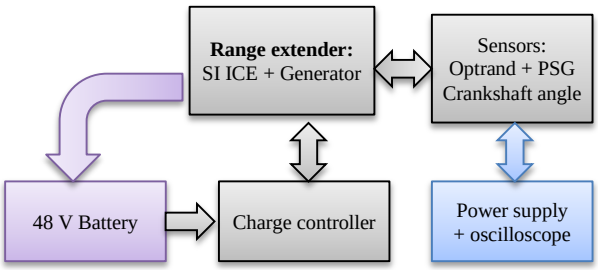

Fig. 6. Test stand block diagram

Data processing has been conducted on a PC with MATLAB software.

3. Sensor response analysis

To compare the two outputs of the sensors, two fuels were used – RON 95 gasoline and a solvent with a significantly lower RON than gasoline. The solvent used for research is a hydrotreated light petroleum fraction (light gasoline). Several test runs were conducted, at varying engine speeds and charge currents. Between each test run, cart electric loads were operated to discharge the battery, and thus, equalize tests conditions.

Figures 7 and 8 show two examples of smoothed sensor readouts. Raw data has been smoothed with the use of a built-in MATLAB function, based on local regression using weighted linear least squares and a 2nd degree polynomial model. This process has been done to facilitate the data processing, while maintaining key signal characteristics, i.e., dynamics and local maxima.

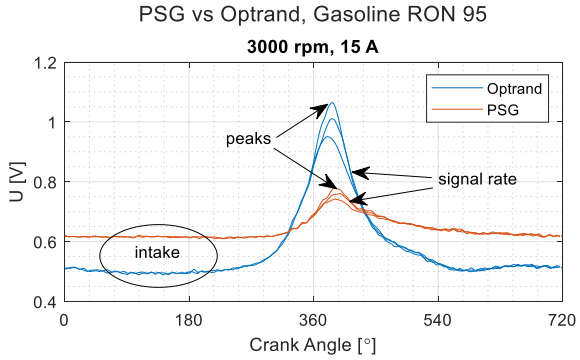

Fig. 7. Sensor response comparison – RON95 gasoline run

The key is to determine the pressure in both the intake phase, as well as in the most crucial, combustion phase. The figures show that for both fuels the PSG sensor readout is significantly weaker, and the sensor response for increasing pressure is slightly delayed by ~3°CA degrees. Additionally, the post-peak signal level tends to drop at a slower rate for the PSG compared to the optical sensor.

In Fig. 7 and 8 it can be observed that there are multiple pressure readouts – for a single measurement multiple engine cycles were observed, and thus, pressure pulses. After recalculating them into the crank angle domain, they all appear in the same spot on the crank angle axis.

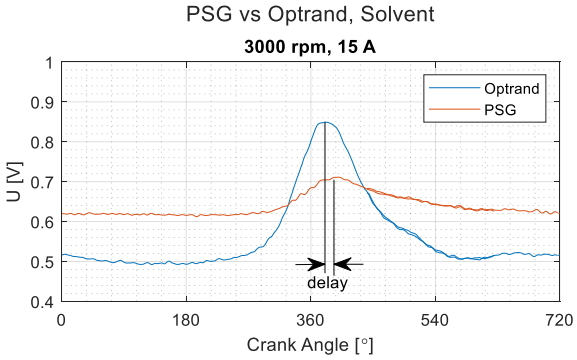

Fig. 8. Sensor response comparison – solvent run

3.1. Test methodology

Since the PSG sensor datasheet is proprietary to its manufacturer, the following approach to convert the voltage values to pressures was proposed. For each fuel, a transfer function

$$U = a_{fuel} \cdot U_{PSG} + b_{fuel} \quad (1)$$

can be determined, according to which the pressure reading from the PSG sensor is recalculated to the voltage levels of the Optrand sensor. The transfer function has been chosen so that the signals correspond to each other in the intake phase (≈ atmospheric pressure), as well as the peak pressure phase.

Firstly, the intake phase signal level from both sensors at 100°CA was extracted. Next, the peak pressure signal levels were noted down. Using the two pairs, both a_{fuel} and b_{fuel} coefficients were determined for each data series. In case a test run possessed multiple pressure peaks, the first peak and a preceding intake phase were considered.

Figure 9 shows the data points used for the recalculation. In this case, the two higher peaks that are visible in both plots, have occurred later in time than the marked ones and were omitted.

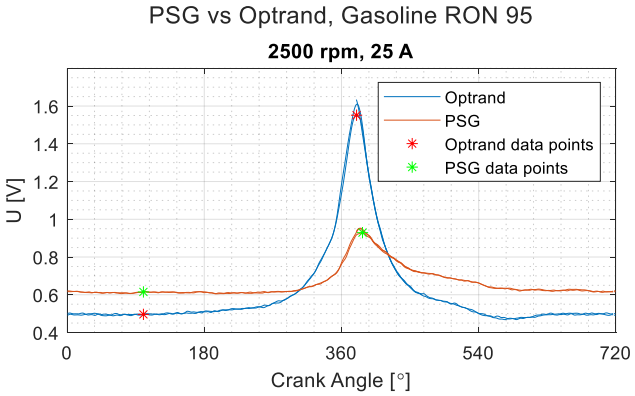

Fig. 9. Example of data with selected points used for signal recalculation

3.2. Sensor voltage recalculation

The recalculation of the coefficients for a variety of test runs (between 1500 and 3500 rpm, and 10 to 25 A of load current) proved that the coefficients form into planes in relation to both parameters, as seen in Fig. 10 and 11 in the form of blue asterisks.

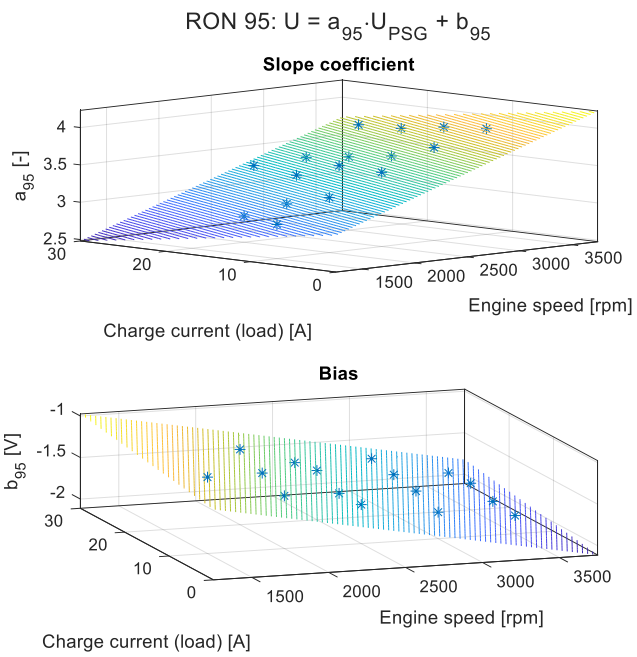

Fig. 10. Approximated coefficient maps for RON95 gasoline

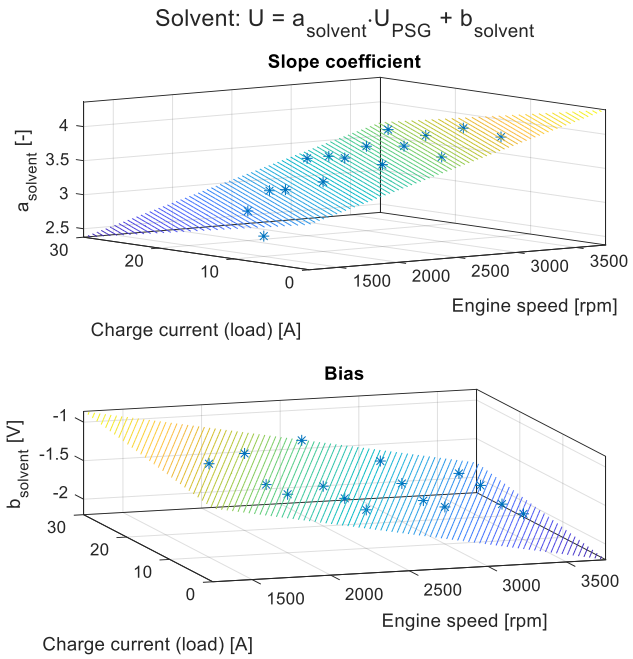

Fig. 11. Approximated coefficient maps for solvent fuel

Hence, it was assumed that coefficients a_{fuel} and b_{fuel} are linear functions of the engine speed and the engine load, expressed in the charge current of the battery.

Using the least squares method, two planes were identified, corresponding to a_{fuel} and b_{fuel} coefficients, and their equations are as follows:

$$a_{95} = 5.03 \cdot 10^{-4} \cdot n - 0.0164 \cdot I_c + 2.35 \quad (2)$$

$$b_{95} = -3.39 \cdot 10^{-4} \cdot n + 0.0096 \cdot I_c - 0.84 \quad (3)$$

$$a_{solvent} = 5.29 \cdot 10^{-4} \cdot n - 0.0221 \cdot I_c + 2.38 \quad (4)$$

$$b_{solvent} = -3.80 \cdot 10^{-4} \cdot n + 0.0130 \cdot I_c - 0.78 \quad (5)$$

The planar approximations have the following coefficients of determination: 0.9306, 0.9143, 0.8044 and 0.7893.

The calculated planes have been depicted in each plot in Fig. 10 and 11 in the form of contour lines.

By obtaining the planar function equations, the PSG sensor readouts could be calculated for any running condition, without the necessity of recording a measurement from the reference sensor. This assumption is only valid within the range of tested charge currents and engine speeds.

4. Results

The method proves to be satisfactorily accurate to recalculate the pressure signal from a pressure-sensing glow plug to Optrand pressure signal levels.

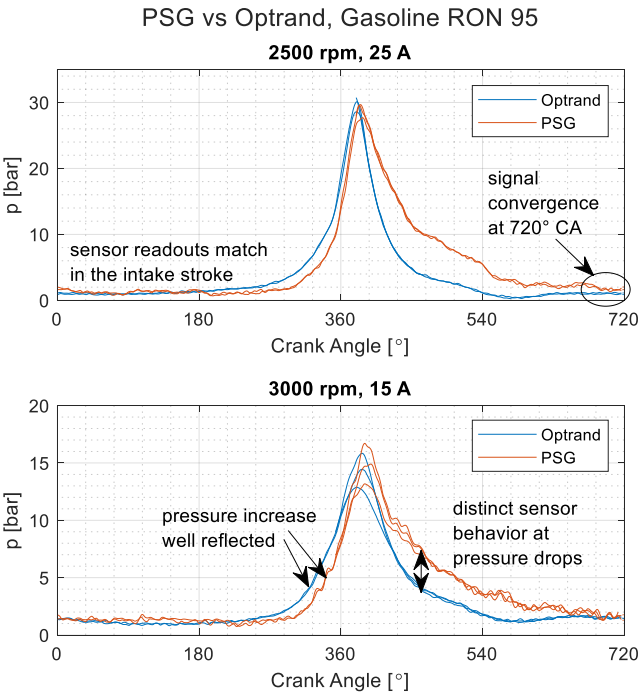

Fig. 12. Recalculated signals for RON95 gasoline

In Fig. 12, it can be visible that both the intake as well as the peak pressure correspond well to each other from both sensor readouts.

Results from the solvent run prove to be satisfactory as well. However, due to poorer coefficients of determination, less accurate signal recalculations can be observed.

In Fig. 13, it can be observed that for the run at 2500 rpm with a 25 A charge current, the intake pressure is poorly reflected. Similar artifacts were observed for both fuels for most outlying runs from the calculated planes, for lowest engine speed and charge current set, i.e., 1500 rpm and 10 A.

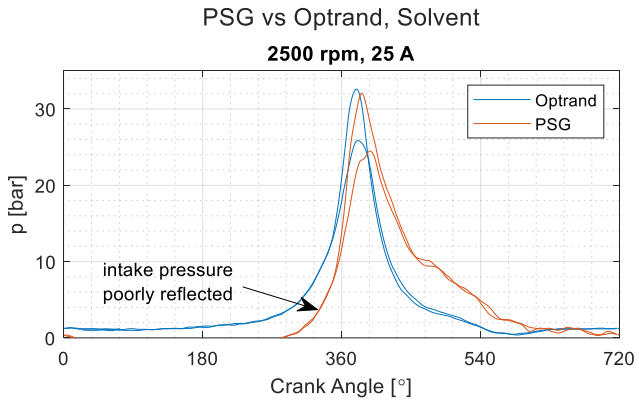

Fig. 13. Recalculated signals for solvent run

As for the sensor comparison, after the recalculation, it can be observed that the pressure reading from the PSG is slower to drop after peak pressure is achieved, which was not clearly visible before recalculation. The sensor readouts converge at the end of the exhaust stroke, around 720°CA.

5. Conclusions

The method proves to be suitable for recalculating the PSG sensor readouts to known Optrand sensor voltage levels. During the tests, it was revealed that the sensitivity of the pressure-sensing glow plug depends on the load and engine speed. It was also shown that the value of the signal also depends on the rate of pressure rise, which was increased by using fuel with a low octane number. The collected data shows that there is a linear dependency between both sensor readouts of different working principle, which can be approximated by planar equations in the domain of engine load and engine speed.

However, the analysis of the results of the tests carried out allowed for obtaining systematized transition functions from the measured PSG signal to the actual value of the pressure measured in the cylinder. This confirms the possibility of using an affordable PSG sensor to control the combustion process in a hydrogen engine. It should be noted that the obtained relationships are preliminary, confirming only the initial assumptions.

To use the sensor in a developed control system, a similar calibration must be performed on the target engine. This is due to the fact that the load carried out on the test stand was measured as the generator charging current and cannot be directly transposed to, for example, the brake mean indicated pressure for the engine.

Nomenclature

AC alternating current
BTDC before top dead center
PSG pressure-sensing glow plug
RON research octane number
SI spark ignition

Bibliography

[1] Al-Dabbas MA, Al-Rousan AA. The simulation of using hydrogen in gasoline internal combustion engines. Pacific Journal of Science and Technology. 2009;10(1):93-106.
[2] Balasubramanian D, Annamalai M. A study on performance, combustion and emission behaviour of diesel engine powered by novel nano nerium oleander biofuel. J Clean Prod. 2018;196:74-83. https://doi.org/10.1016/j.jclepro.2018.06.002
[3] Bondarenko I, Lukoševičius V, Keršys R Neduzha L. Investigation of dynamic processes of rolling stock–track interaction: experimental realization. Sustainability. 2023;15:5356. https://doi.org/10.3390/su15065356
[4] Chłopek Z, Stasiak P. The analysis of an unrepeatability of cylinder pressure signal in internal combustion engines. Combustion Engines. 2005;120(1):31-39. https://doi.org/10.19206/CE-117409
[5] Gis M, Gis W. The current state and prospects for hydrogenisation of motor transport in Northwestern Europe and Poland. Combustion Engines. 2022;190(3):61-71. https://doi.org/10.19206/CE-144560
[6] Lijewski P, Fuć P, Grzeszczyk R, Molik P, Rymaniak Ł, Ziółkowski A. The use of an integrated combustion chamber sensor for engine cylinder pressure measurement (in Polish). Logistyka. 2014;3:3765-3770.
[7] Longwic R, Tatarynow D, Kuszneruk M, Wozniak-Borawska G. Preliminary tests of a Diesel engine powered by diesel and hydrogen. Combustion Engines. 2023;195(4):35-39. https://doi.org/10.19206/CE-169485
[8] Matla J. Possible applications of prechambers in hydrogen internal combustion engines. Combustion Engines. 2022;191(4):77-82. https://doi.org/10.19206/CE-148170
[9] Menes M. Program initiatives of public authorities in the field of hydrogenation of the economy in a global perspective, as of the end of 2020. Combustion Engines. 2022;189(2):18-29. https://doi.org/10.19206/CE-142170
[10] New glow plug technology from the world market leader. BERU Technical briefs. Available from: https://www.beruparts.eu/content/dam/marketing/emea/beru/brochure/en-psg-pressure-sensor-glow-plug.pdf
[11] Noga M. Selected issues of the indicating measurements in a spark ignition engine with an additional expansion process. Appl Sci. 2017;7(3):295. https://doi.org/10.3390/app7030295
[12] Noga M, Gorczyca P. Development of the range extender for a 48 V electric vehicle. Combustion Engines. 2019;177(2):113-121. https://doi.org/10.19206/CE-2019-220
[13] Noga M, Gorczyca P, Hebda R. The effects of use of the range extender in a small commercial electric vehicle. Automotive Experiences. 2021;4(1):5-19. https://doi.org/10.31603/ae.4137
[14] Pavelčík V, Dižo J, Blatnický M, Ishchuk V, Molnár D. Analysis of the test bench design influence on the cooling performance of a rail vehicle brake disc. Communications – Scientific Letters of the University of Žilina. 2023;25(2):194-200. https://doi.org/10.26552/com.C.2023.048
[15] Pielecha I, Wierzbicki S, Sidorowicz M, Pietras D. Combustion thermodynamics of ethanol, n-heptane, and n-butanol in a Rapid Compression Machine with a Dual Direct Injection (DDI) supply system. Energies. 2021;14:2729. https://doi.org/10.3390/en14092729
[16] Stępień Z. Synthetic automotive fuels. Combustion Engines. 2023;192(1):78-90. https://doi.org/10.19206/CE-152526

[17] Szczurowski K, Walczak D, Zieliński Ł. Use of pressure sensor glow plug for the control of combustion process (in Polish). Zeszyty Naukowe Instytutu Pojazdów. 2014;99: 139-144.
[18] Szwaja S. Combustion pressure fluctuations study in the hydrogen fueled internal combustion engine (in Polish). Częstochowa University of Technology Publishing House. Częstochowa 2010.
[19] Szwaja S, Szymkowiak M. The Szymkowiak's over-expanded cycle in the rocker engine with the variable compression ratio – kinematics. Combustion Engines. 2022; 189(2):68-72. https://doi.org/10.19206/CE-143157
[20] Vollberg D, Wachter D, Kuberczyk T, Schultes G. Cylinder pressure sensors for smart combustion control. Journal of Sensors and Sensor Systems. 2019;8:75-85. https://doi.org/10.5194/jsss-8-75-2019
[21] Wesołowski M, Hamid M, Mońka P, Janicka A. Analysis of the potential of electro-waste as a source of hydrogen to power low-emission vehicle powertrains. Combustion Engines. https://doi.org/10.19206/CE-169494

Marcin Noga, DSc., DEng. – Faculty of Mechanical Engineering, Cracow University of Technology, Poland.
e-mail: *marcin.noga@pk.edu.pl*

Tomasz Moskal, MEng. – Faculty of Mechanical Engineering, Cracow University of Technology, Poland.
e-mail: *tomasz.andrzej.moskal@gmail.com*